HEATING-INDUCED FLOWS IN CABLE-IN-CONDUIT CONDUCTORS*

Lawrence Dresner

Fusion Energy Division

Oak Ridge National Laboratory
Oak Ridge, Tennessee 37830

*Research sponsored by the Office of Fusion Energy, U.S. Department of under contract W-7405-eng-26 with the Union Carbide Corporation.

Heating-Induced Flows in Cable-in-Conduit Conductors

Lawrence Dresner
Fusion Energy Division
Oak Ridge National Laboratory, Oak Ridge, TN 37830

1. Introduction

Hoenig et al[1] and Miller et al[2] have both reported high stability margins for cable-in-conduit conductors cooled by stationary supercritical helium. Miller et al proposed that strong flows induced in the helium in the early stages of recovery enhanced heat transfer and greatly increased the stability margin over what had been expected for stationary helium. In this memorandum, we calculate the flow and pressure transients induced in initially stationary helium by energy transfers typical of those associated with conductor recovery (50-200 mJ cm^{-3} in 10-20 msec).

2. Basic Equations

In order to calculate the heating-induced flow in supercritical helium, we start with the one-dimensional theory of compressible flow:[3]

(1a) $$\frac{\partial \rho}{\partial t} + \rho \frac{\partial v}{\partial x} + v \frac{\partial \rho}{\partial x} = 0 \quad \text{(continuity)}$$

(1b) $$\rho \frac{\partial v}{\partial t} + \rho v \frac{\partial v}{\partial x} + \frac{\partial p}{\partial x} = 0 \quad \text{(momentum)}$$

where ρ is the density of the helium, v is its flow velocity, and p is its pressure. We linearize the theory by dropping the second-order terms underlined by dashed lines. Such linearization is allowable if the induced velocity $\ll C$, the velocity of sound, and the induced transient pressure $p \ll \rho C^2$. At 4.0K and 5.0 atm., $C = 246$ ms^{-1}, $\rho = 144$ kg m^{-3}, and $\rho C^2 = 87.1$ atm. We shall check that $v \ll C$ and $p \ll \rho C^2$ after we estimate v and p and thus justify use of the linear theory.

The energy equation can be written

(2) $$\rho \frac{d}{dt}\left(\frac{1}{2} v^2 + e\right) = -\frac{\partial}{\partial x}(pv) + \rho \frac{dq}{dt} \quad \text{(energy)}$$

where e is the internal energy per unit mass of helium, q is the heat

input per unit mass of helium, and d/dt is the hydrodynamic derivative, equal to $\partial/\partial t + v\partial/\partial x$. After linearization, (2) becomes

$$\rho \frac{\partial e}{\partial t} + p \frac{\partial v}{\partial x} = \rho \frac{\partial q}{\partial t} \tag{3}$$

If we substitute from (1a) for $\partial v/\partial x$, we get

$$\frac{\partial q}{\partial t} = \frac{\partial e}{\partial t} - \frac{p}{\rho^2} \frac{\partial \rho}{\partial t} \tag{4a}$$

$$= \frac{\partial e}{\partial t} + p \frac{\partial \tau}{\partial t} \tag{4b}$$

$$= T \frac{\partial s}{\partial t} \tag{4c}$$

where $\tau = \rho^{-1}$ is the specific volume of helium, and s is entropy per unit mass. To pass from (4b) to (4c) we use the first and second laws of thermodynamics in the form $Tds = de + pd\tau$.

With (4) established, we proceed to eliminate the derivatives of ρ from (1a,b) using the thermodynamic identity

$$d\rho = \left(\frac{\partial \rho}{\partial p}\right)_s dp + \left(\frac{\partial \rho}{\partial s}\right)_p ds \tag{5a}$$

which can be written

$$\frac{\partial \rho}{\partial t} = \frac{1}{c^2} \frac{\partial p}{\partial t} + \left(\frac{\partial \rho}{\partial s}\right)_p \frac{\dot{q}}{T} \tag{5b}$$

since $c^2 \equiv (\partial p/\partial \rho)_s$. Substituting (5b) into (1a) we find it can be written

$$\frac{1}{c_o^2} \frac{\partial p}{\partial t} + \rho_o \frac{\partial v}{\partial x} = - \left(\frac{\partial \rho}{\partial s}\right)_p \frac{\dot{q}}{T} \tag{6a}$$

where the subscript zero refers to the properties of unperturbed (ambient) helium. Rewriting (1b) we have

$$\rho_o \frac{\partial v}{\partial t} + \frac{\partial p}{\partial x} = 0 \tag{6b}$$

If we divide (6b) by ρ_o, multiply (6a) by C_o/ρ_o, and then add (6a) to or subtract it from (6b), we get

$$(7a)\quad \frac{\partial}{\partial t}\left(v + \frac{p}{\rho_o C_o}\right) + C_o \frac{\partial}{\partial x}\left(v + \frac{p}{\rho_o C_o}\right) = -\frac{C_o}{\rho_o}\left(\frac{\partial \rho}{\partial s}\right)_p \frac{\dot{q}}{T} = \frac{C_o}{\tau_o}\left(\frac{\partial v}{\partial s}\right)_p \frac{\dot{q}}{T}$$

$$(7b)\quad \frac{\partial}{\partial t}\left(v - \frac{p}{\rho_o C_o}\right) - C_o \frac{\partial}{\partial x}\left(v - \frac{p}{\rho_o C_o}\right) = \frac{C_o}{\rho_o}\left(\frac{\partial \rho}{\partial s}\right)_p \frac{\dot{q}}{T} = -\frac{C_o}{\tau_o}\left(\frac{\partial v}{\partial s}\right)_p \frac{\dot{q}}{T}$$

Because p only appears as the argument of a derivative, we can interpret it now as the pressure rise. Eqs. (7a,b) are the characteristic equations; from them it follows that

(8) $v \pm \frac{p}{\rho_o C_o}$ increases by $\pm \frac{C_o}{\tau_o}\left(\frac{\partial v}{\partial s}\right)_p \frac{\dot{q}}{T} \Delta t$ as we traverse a segment of the characteristic $x \pm C_o t$ = constant that spans the time interval Δt.

3 Special Units

It will prove convenient in what follows to choose the units of mass, length, and time so that the quantities C_o, $\rho_o C_o$, and $a_o = \frac{C_o}{\tau_o}\left(\frac{\partial v}{\partial s}\right)_p \frac{\dot{q}}{T}$ all equal 1. There the statement (8) can be written

(9a) $v \pm p$ increases by $\pm \Delta t$ as we traverse a segment of the characteristic $x \pm t$ = constant that spans the time interval Δt

(9a) applies only in the presence of the heat source $\dot{q}$. In zones that are not externally heated, (8) becomes

(9b) $v \pm p$ is constant along the characteristic $x \pm t$ = constant.

In order to return from the special units to mks units, we need to know the values of ρ_o, C_o, and a_o. ρ_o and C_o are tabulated directly in

NBS-631. Since $T\left(\partial s/\partial t\right)_p = \left(\partial h/\partial t\right)_p$,

$$a_o = \frac{C_o \dot{q}}{T_o\left(\frac{\partial h}{\partial t}\right)_p} \tag{10}$$

the denominator of which is also tabulated in NBS-631.

It is worth noting at this point that we have not invoked any equation of state for the helium, so that our results apply even near the critical point (except that $p \ll \rho_o C_o^2$ and $v \ll C_o$).

4. Wave Diagram

We can use the statements (9a) and (9b) to calculate the space-time dependence of the velocity and pressure in an infinite tube with a finite heated section using the wave diagram, Fig. 1. The axes of the wave diagram are space (abscissa) and time (ordinate). Lines in the wave diagram therefore represent trajectories. In the special units we are using, lines of slope ± 1 represent forward and backward trajectories of points moving with sonic velocity (positive and negative characteristics). The segment P'P of the x-axis represents the heated section of the tube. The area between the vertical dashed lines represents the region of space-time for which $\dot{q} > 0$. In this region, statement (9a) holds; outside of it, statement (9b) holds. At the outset ($t=0$, i.e., along the x-axis), $v = p = 0$ (remember, that p is now the pressure rise).

Let us now calculate the distribution of velocity and pressure rise at a time $t > 0$, i.e., along the horizontal line with ordinate t. We begin with the point A which lies at the intersection of the horizontal line and the positive characteristic emanating from P. Because the segment PA of the characteristic lies outside the dotted lines, we can apply statement (9b) to find that

$$v_A + p_A - v_p - p_p = 0 \tag{11a}$$

or

$$v_A + p_A = 0 \tag{11b}$$

since $v_p = p_p = 0$. Similarly, by applying (9b) to the negative characteristic QA through A we find

$$v_A - p_A = 0 \tag{12}$$

so that $v_A = p_A = 0$.

We can make a similar calculation for point B:

(13a) $v_B + p_B = t$ (positive characteristic; 9a)

(13b) $v_B - p_B = 0$ (negative characteristic; 9b)

so that $v_B = p_B = t/2$.

At any point C between A and B, we have

$$\left.\begin{aligned} &(14a) \quad v_C + p_C = t' \\ &(14b) \quad v_C - p_C = 0 \end{aligned}\right\} \quad v_C = p_C = t'/2$$

where t' is the time interval the positive characteristic through C spends in the heated zone. Now $t'/t = AC/AB$, so that v_C and p_C vary linearly with distance between A and B. Such linear behavior is characteristic of the particular problem we are solving. It can be shown without too much difficulty that (i) the profiles of velocity and pressure rise are composed of straight line segments, and (ii) that segments of different slope can only intersect at points at which either the head or tail of one of the characteristics leaves or enters the heated zone.

At point D,

$$\left.\begin{aligned} &(15a) \quad v_D + p_D = t \\ &(15b) \quad v_D - p_D = -t \end{aligned}\right\} \quad \begin{aligned} v_D &= 0 \\ p_D &= t \end{aligned}$$

and these equations are evidently true for all points between E and D. Figs. 2a and 2b show the pressure and velocity profiles we have just calculated. If the reader has not already realized it, these profiles hold for time $t < \ell/2$, where ℓ is the length of the heated section.

For $\ell/2 < t < \ell$, we use the wave diagram in Fig. 3. Again $v_A = p_A = 0$ and $v_B = p_B = t/2$. At point D, $v_D = t - \ell/2$, $p_D = \ell/2$. At point E, $v_E = 0$, $p_E = \ell/2$. The pressure and velocity profiles are shown in Fig. 4a and 4b. For $\ell < t < 3\ell/2$, we use the wave diagram in Fig. 5. Then, $v_A = p_A = 0$, $v_B = p_B = \ell/2$, $v_C = p_C = \ell/2$, and $v_E = 0$, $p_E = \ell/2$. The pressure and velocity profiles are shown in Fig. 6a and 6b. For times $t > \ell$, the wave diagram, and the pressure

and velocity profiles are like those of Figs. 5 and 6 except that points A and B move rightwards at sonic velocity.

In obtaining this solution, we have assumed the heat source $\dot{q}$ to be present in the tube section P'P. If $\dot{q}$ ever becomes zero in section P'P, it means the superconductor has recovered, and we need not follow the flow and pressure transient further. This explains why we do not consider late stages of the flow and pressure transient for which $\dot{q}$ may be zero.

5. Analysis of the Experiments of Miller et al

In the experiments of Miller et al., a 1.52-m-long triplex in a stainless steel tube was driven normal by an embedded heater. The hydrodynamic conditions of this experiment do not conform with the calculation just performed because the ends of the test section communicate with large helium reservoirs rather than with unheated tubes of equal diameter. To analyze Miller's experiment we can only consider the portions of the earlier wave diagrams between the dotted lines. On the dotted lines we add the boundary condition $p = 0$ since there can be no pressure rise in the reservoirs. (In other words, the three-dimensional spreading of the pressure wave in the reservoir causes the pressure to fall rapidly as we move away from the mouth of the heated tube.) The new wave diagram is shown in Fig. 7.

Consider a time $t < 2/2$. At point A, $v_A + p_A = t$ (positive characteristics; 9a). But since $p_A = 0$, $v_A = t$. For point B, we have

(16a) $$v_B + p_B = t$$

(16b) $$v_B - p_B - (v_{B'} - p_{B'}) = - t_{AB'}$$

(16c) $$p_{B'} = 0 \quad ; \quad v_{B'} = t_{B''B'}$$

or

(16d) $$v_B = \frac{1}{2} (t - t_{AB'} + t_{B'B''}) = t_{B'B''}$$

(16e) $$p_B = \frac{1}{2} (t + t_{AB'} - t_{B'B''}) = t_{AB'}$$

From these equations it follows that $v_C = 0$ and $p_C = t$ and that both v and p vary linearly from A to C. The pressure and velocity profiles are presented in Fig. 8.

We can advance further in time in this problem by deriving simple formulas that will allow us to calculate velocity and pressure profiles from those for times $\ell/2$ or ℓ earlier. We use the wave diagrams in Fig. 9. Section 1 shows two points, C and A, at two times an interval $\ell/2$ apart. The points are symmetrically located with respect to the quarter point of the heated section. Using the boundary conditions that $p = 0$ at the ends of the heated section and $v = 0$ at its midpoint, we find after a short calculation

$$\left.\begin{aligned} (17a) \qquad v_C &= p_A + \frac{\ell}{2} - x_A \\ (17b) \qquad p_C &= x_A - v_A \end{aligned}\right\} \quad \begin{aligned} t_C - t_A &= \ell/2 \\ x_C &= \ell/2 - x_A \end{aligned}$$

where x_A is the distance of point A from the midpoint. Graphically, the meaning of (17a) is as follows: To the pressure distribution at time t_A we add $\ell/2 - x_A$, which is the line of slope -1 passing through the end of the heated zone. Then we reflect the sum around the quarter point. The result is v_C. The graphical meaning of (17b) is to subtract the velocity profile at t_A from x_A (the line of slope 1 through the midpoint) and then reflect about the quarter point. The result is p_C.

Two applications of (17) or a direct computation from section 2 of Fig. 9 gives

$$\left.\begin{aligned} (18a) \qquad p_D &= - p_A \\ (18b) \qquad v_D &= 2x_A - v_A \end{aligned}\right\} \quad \begin{aligned} t_D - t_A &= \ell \\ x_D &= x_A \end{aligned}$$

The meaning of (18a) is clear; the graphical meaning of (18b) is as follows: To get the velocity profile at time t_D, subtract the velocity profile at time t_A from the line of slope 2 through the midpoint.

Shown in Fig. 10 are pressure and velocity profiles at times $3\ell/8$, $7\ell/8$, $11\ell/8$, and $15\ell/8$. After a time 2ℓ, the process repeats, and continues to repeat as long as the heat source is present. The velocity averaged over the length of the heated section and over a full cycle is $\ell/4$, i.e., one-quarter of the maximum velocity. It is this average which should be significant in determining the average heat transfer in the experiments of Miller et al.

7. Evaluation of Pressure Rise, Induced Velocity, and Heat Transfer

The maximum induced pressure rise and flow velocity are given in special units by $v_{max} = \ell$ and $p_{max} = \ell/2$. In ordinary units,

$$v_{max} = \frac{a_o \ell}{C_o} \tag{19a}$$

$$p_{max} = \rho_o a_o \left(\frac{\ell}{2}\right) \tag{19b}$$

At 5.0 atm and 4.2 K, the conditions of the experiment, $\rho_o = 141$ kg m^{-3}, $C_o = 240$ m s^{-1}, and $\tau(\partial h/\partial T)_p = 40.1$ J g^{-1}. At 200 A transport current, the total heat addition to the helium was about 3.4 J g^{-1}. The recovery time was $\sim$ 50 msec, but for nearly half of that time, the conductor temperature was between the critical and current-sharing temperatures (6.0 K, 5.1 K, respectively). As a best guess, we take $\dot{q} = 100$ W g^{-1}. Thus $a_o = 600$ m s^{-2}, $v_{max} = 3.80$ m s^{-1}, and the average induced velocity $\langle v \rangle = 0.95$ m s^{-1}. The corresponding maximum pressure rise is 0.64 atm.

The hydraulic diameter D is 0.4 mm, and the kinematic viscosity is 2.9×10^{-8} m^{2}s^{-1}. The average Reynolds number Re of the induced flow is then 13000. Using a Prandtl number Pr = 0.6 for helium at 4.2 K and 5.0 atm we can estimate the Nusselt number Nu from the steady-state Dittus-Boelter-Giarratano correlation: $Nu = 0.026\ (Re)^{0.8}\ (Pr)^{0.4} = 42$. With a thermal conductivity k of helium of 0.022 Wm^{-1}K^{-1}, we find the average heat transfer coefficient during recovery $h = k(Nu)/D = 2300$ Wm^{-2}K^{-1}. The corresponding heat transfer coefficient deduced from the measured stability margin is 850 Wm^{-2}K^{-1}.

8. Discussion

The main uncertainties in the "hydrodynamic" value of h just obtained here arise from (i) the tacit assumption of steady heat input (i.e., constant $\dot{q}$) during recovery and (ii) the use of the steady-state correlation between flow and heat transfer. The main uncertainty in the "stability" value of h is due to its being derived under the assumption of constant thermophysical properties. These uncertainties make the comparison of these two numbers a dubious way of checking how right our picture of recovery at zero flow is. Probably the best way of comparing the theory presented here with experiment is to measure the time variation of the pressure at selected points along the sample. Pressure oscillations of the type predicted in Fig. 10b

have already been seen in as yet unreported experiments carried out in a 3-m-long tube, but the boundary conditions at the ends of the tube do not conform well with those underlying Fig. 10b so that quantitative comparison of the amplitude and period is not possible.

The work presented here has some important implications regarding how the stability margin at zero imposed flow varies with (i) the length of the heated section (normal zone) and (ii)the boundary conditions imposed at the ends of the heated section. The second factor can make a difference between the stability margin of a conductor in a short-sample test and the stability margin of the same conductor when wound into a coil. The first factor can make a difference between the stability margin when a short length of conductor is driven normal (as in a short-sample test) and the stability margin in a large coil when, say, half a turn is driven normal. Half a turn of an LCP coil is about 6m long. According to the calculations summarized in section 4, the helium velocity in the center 50-cm-long section remains zero for about 12 msec, whereas if the same 50-cm-long center section is part of a 1-m-long short sample test, the velocity remains zero there for only 2 msec. These considerations indicate the need for experimental study of stability at zero imposed flow as a function of the length of the heated zone and of how the heated zone is connected to the rest of the helium.

References

1. M. O. Hoenig and A. G. Montgomery, Proc. Seventh Symposium on Engineering Problems of Fusion Research, IEEE Pub. No. 77CH1267-4-NPS, Oct., 1977, p. 780; M. O. Hoenig, A. G. Montgomery, and S. J. Waldman, Applied Superconductivity Conference, Pittsburgh, PA, Sept. 25-28, 1978; A. G. Montgomery and M. O. Hoenig, ibid.

2. J. R. Miller, J. W. Lue, S. S. Shen, and J. C. Lottin, Applied Superconductivity Conference, Pittsburgh, PA, Sept. 25-28, 1978.

3. "Handbook of Physics," E. U. Condon and H. Odeshaw (eds), Part 3, Ch. 4, 'Wave Propagation in Fluids," by A. H. Taub, McGraw-Hill, NY, 1967.

ORNL-DWG 79-2170 FED

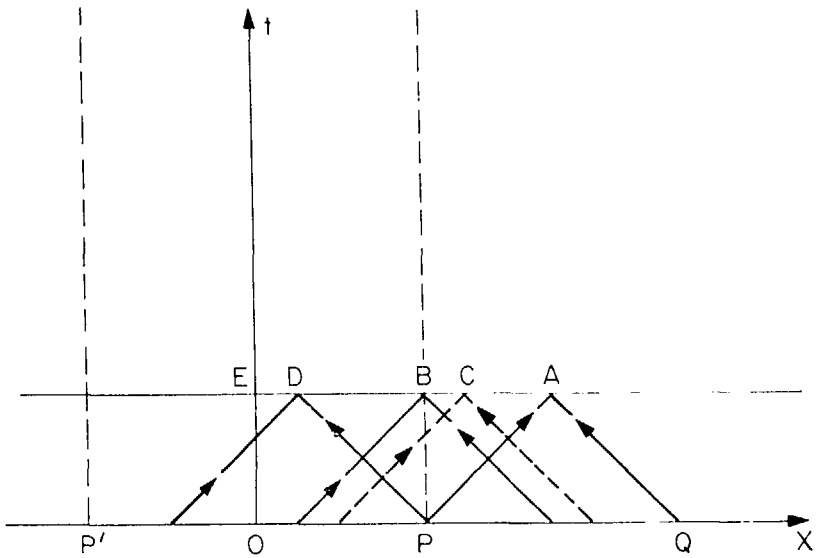

WAVE DIAGRAM

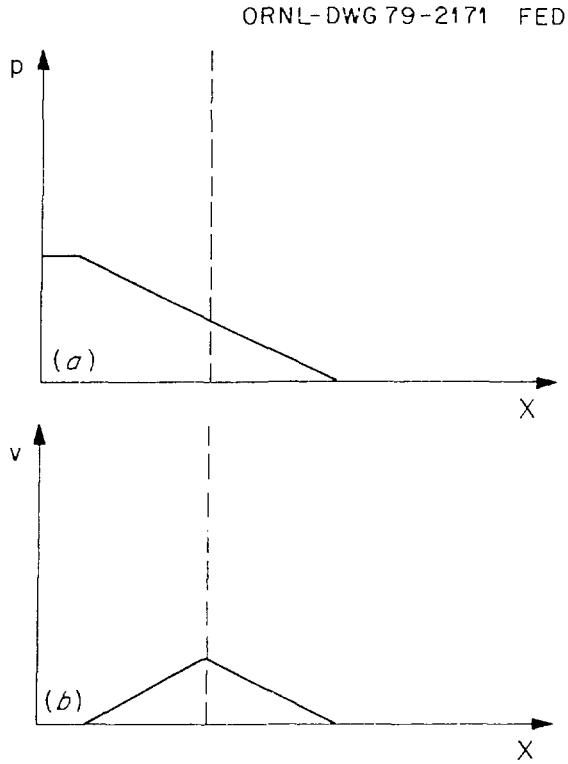

VELOCITY AND PRESSURE PROFILES

ORNL-DWG 79-2172 FED

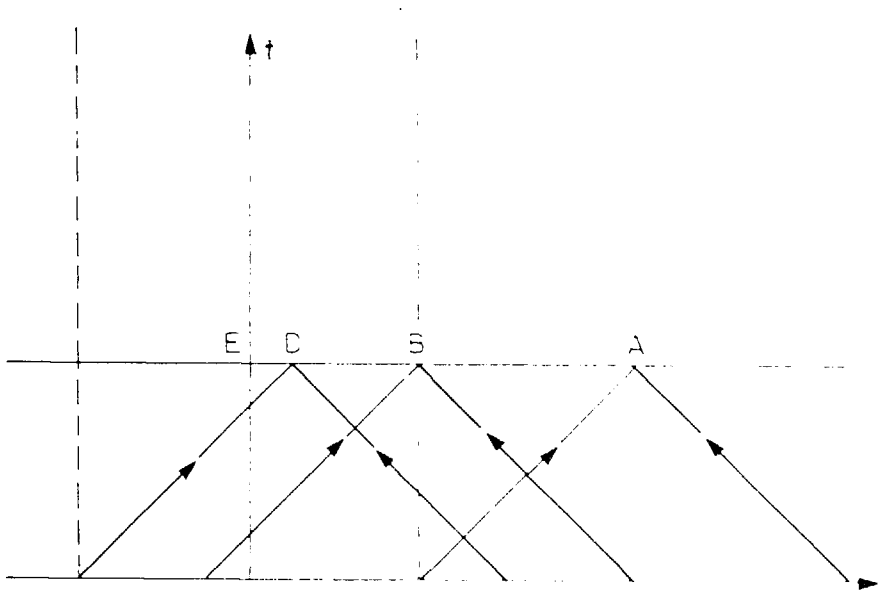

WAVE DIAGRAM

ORNL-DWG 79-2173 FED

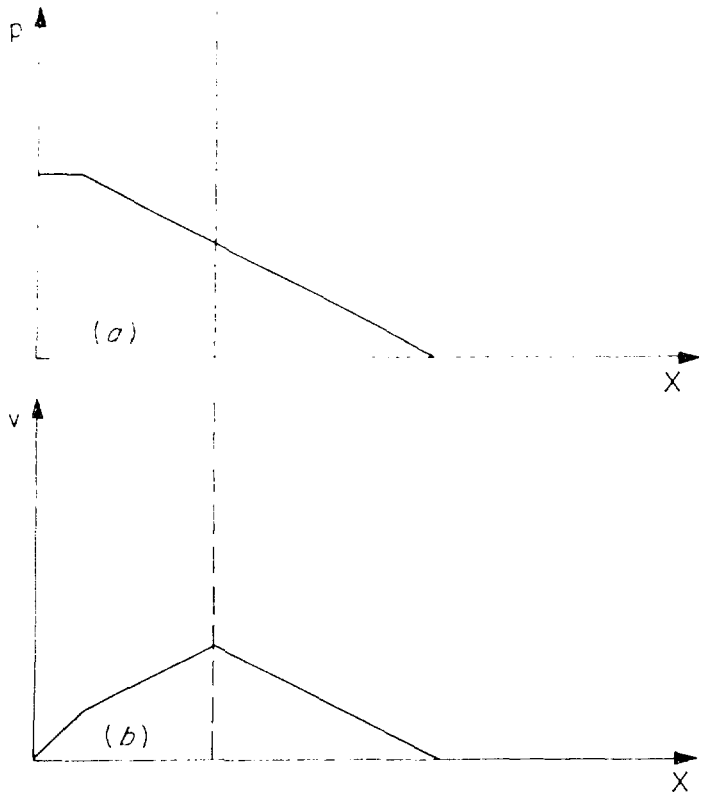

VELOCITY AND PRESSURE PROFILES

ORNL-DWG 79-2174 FED

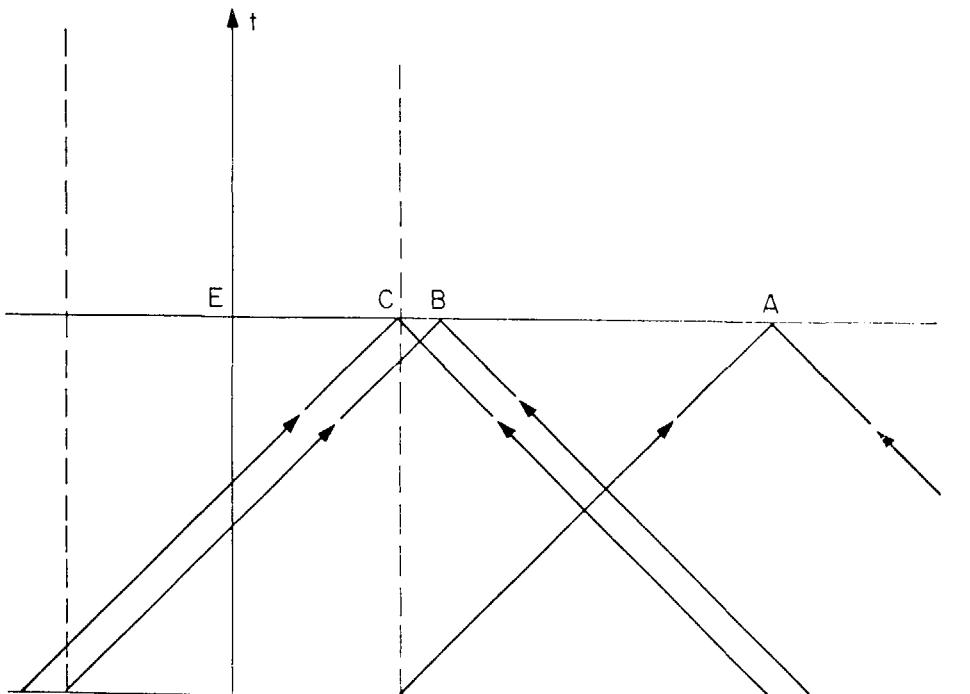

WAVE DIAGRAM

ORNL-DWG 79-2175 FED

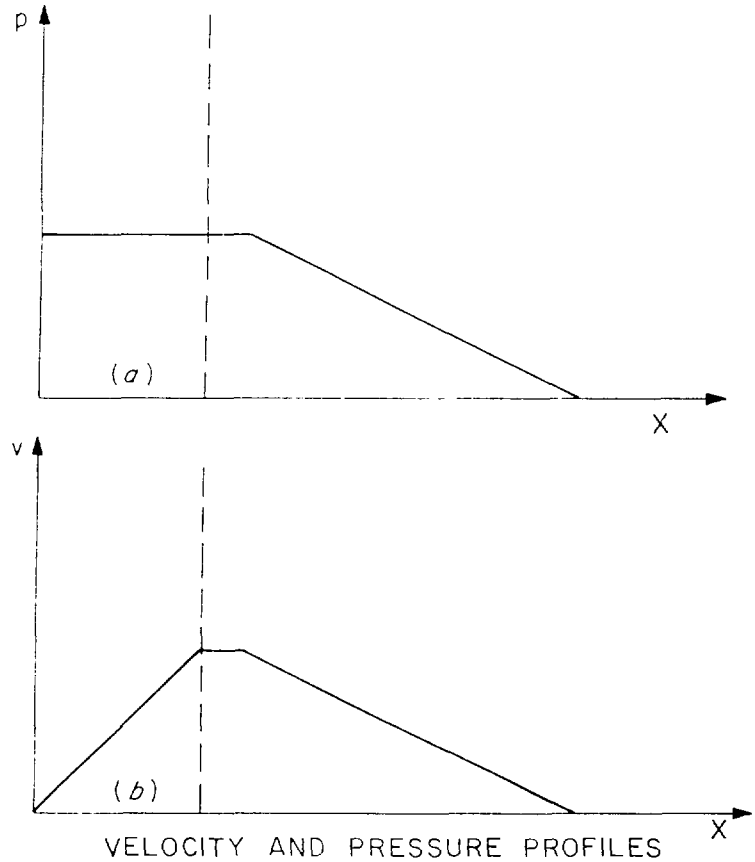

VELOCITY AND PRESSURE PROFILES

ORNL-DWG 79-2176 FED

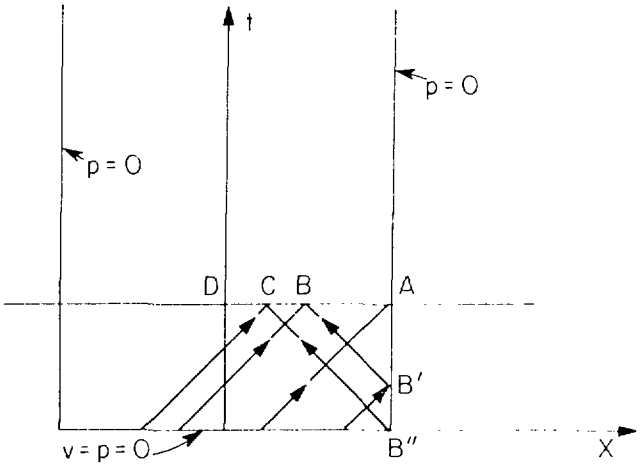

WAVE DIAGRAM

ORNL-DWG 79-2177 FED

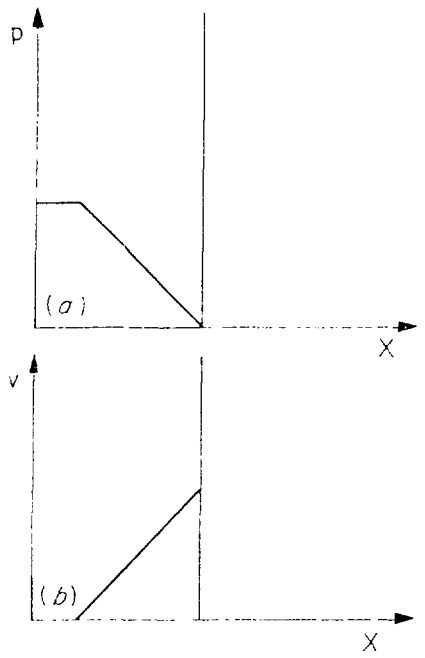

PRESSURE AND VELOCITY PROFILES

ORNL-DWG 73-2178 FED

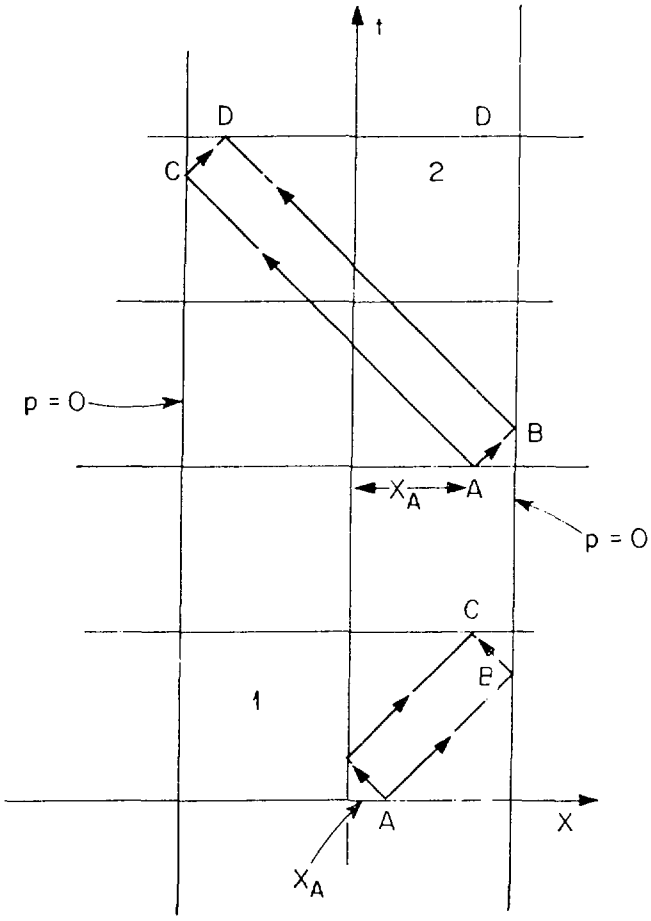

WAVE DIAGRAM

ORNL-DWG 79-2179 FED

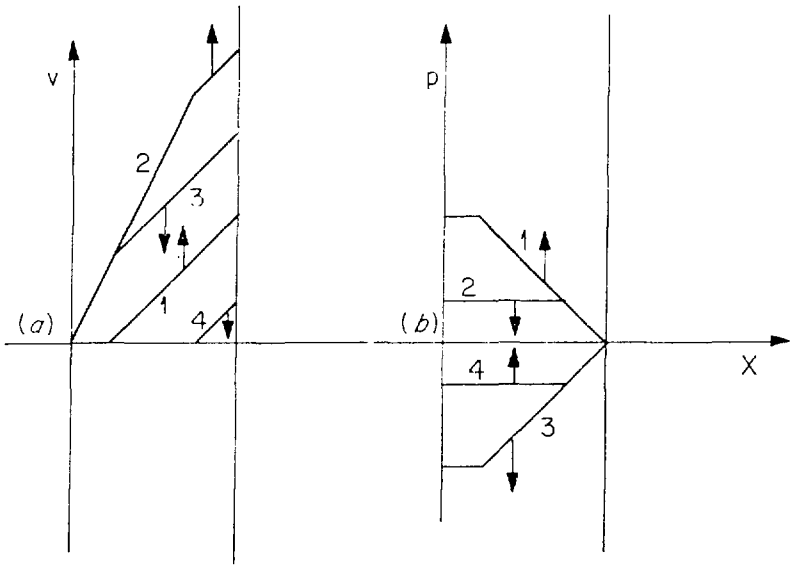

VELOCITY AND PRESSURE PROFILES AT TIME INTERVALS OF $\ell/2$